

Investigation of $2\omega_0$ -harmonic generation in a laser plasma

N. G. Basov, V. Yu. Bychenkov, O. N. Krokhin, M. V. Osipov, A. A. Rupasov, V. P. Silin, G. V. Sklizkov, A. N. Starodub, V. T. Tikhonchuk, and A. S. Shikanov

P. N. Lebedev Institute of Physics, Academy of Sciences of the USSR

(Submitted 25 January 1979)

Zh. Eksp. Teor. Fiz. 76, 2094–2109 (June 1979)

A theoretical model for the generation of the second harmonic of laser radiation in a plasma produced by the radiation is formulated. The main features of this model have been verified experimentally on the "Kal'mar" laser facility in experiments on spherical irradiation of gas-filled microspheres. It is demonstrated that such a model consistently explains the presently available experimental data on second-harmonic generation in a laser plasma. This allows the development of new methods of ultra-high-speed diagnostics of nonstationary overdense plasmas.

PACS numbers: 52.50.Jm, 52.35.Mw

INTRODUCTION

The detection of the second harmonic in the investigations published in Refs. 1–3 was one of the first indications of the manifestation of nonlinear effects in the interaction of laser radiation with the plasma produced by it. Further experiments showed that the coefficient of conversion of the pump energy into the second harmonic was not high (not more than one percent) and, consequently, the emission of the harmonic does not play an important role in the energy balance of the plasma. This, however, did not diminish the interest in the investigation of the harmonics, which is explained by the attempts to use the optical emission of the laser plasma to extract information about the nonlinear processes that occur in the "corona" of the plasma. Considering the large quantity, and, on the face of it, the inconsistency, of the experimental data, we need for an adequate description of the physical processes that occur in the corona of a laser plasma to develop a theoretical model of $2\omega_0$ -harmonic generation. Such a model can, furthermore, serve as a basis for the development of new, laser-plasma-parameter diagnostics methods distinguished by ease of practical realization.

The first theoretical ideas⁴ about the generation of the second harmonic related this effect with the excitation in the plasma of the intense longitudinal oscillations that arise as a result of the linear transformation⁵ of the laser radiation. Qualitatively, another possibility of exciting longitudinal Langmuir waves in a plasma arises at sufficiently high densities of the laser-radiation energy flux, when parametric instabilities develop in the plasma.⁶ Thus, for example, the second-harmonic spectrum broadening observed in Refs. 7 and 8, and characteristic of the turbulent plasma state, was related by the authors of these investigations with the development of parametric turbulence.

Our present understanding of the physical essence of the phenomenon of second-harmonic generation has revealed new possibilities of laser-plasma diagnostics. The first theoretical ideas about the use of the measurements of the spectrum and intensity of the harmonic for the determination of a number of laser-plasma parameters were stated in Refs. 9 and 10. The estimates obtained in Refs. 11–14 for the value of the local temperature and the characteristic dimension of the plasma in-

homogeneity demonstrated the merit of the development of plasma-parameter diagnostics methods based on the use of the plasma emission in the range of frequencies close to the double pump frequency. Let us emphasize that, besides the macroscopic plasma parameters, the investigation of the $2\omega_0$ harmonic allows us to obtain information about the level and spectrum of parametric turbulence. Such a possibility is pointed out in Ref. 15. In their turn, the data on plasma turbulence can be related with the nonlinear-absorption efficiency and fast-particle generation. When we remember that the simultaneous manifestation of the two-linear and nonlinear-mechanisms of generation of longitudinal waves is possible under experimental conditions,^{14,16–18} we can understand why the detailed study of the second harmonic should yield a wealth of information about the plasma state.

In §1 of the present paper we formulate a theoretical model of $2\omega_0$ -harmonic generation in a laser plasma. We derive formulas that allow the computation of the intensity, spectrum, angular, and polarization characteristics of the harmonic for moderate fluxes of the laser radiation. The main assumptions of the model and a number of results following from it are verified experimentally on the multichannel "Kal'mar" laser facility in experiments on spherically-symmetric irradiation of shell targets and compared with hydrodynamic calculations (§2). In §3 we carry out an analysis of virtually all the presently available experimental data on second-harmonic generation. It is shown that the model proposed in the present paper satisfactorily describes the experiments. The plasma-parameter estimates that follow from the comparison of the theory with experiment agree with the measured values. All this is a justification of the new methods of diagnostics of plasma parameters and plasma turbulence from the characteristics of the plasma emission at the frequency of the second harmonic.

§1. THEORY OF SECOND-HARMONIC GENERATION IN A LASER PLASMA

The process of linear conversion of light into longitudinal Langmuir waves is possible in an inhomogeneous plasma near the plasma resonance in the presence of the incident wave of an electric-field vector component directed along the density gradient (the p component).

The intensity of the second harmonic emitted as a result of this process is calculated in Refs. 4, 9, and 19 under the assumption that the density inhomogeneity of the quiescent plasma is one-dimensional [i.e., $n_e = n_e(x)$] and that the incident wave is a plane wave. However, for the interpretation of experiments, it is necessary to take into account such factors as the conditions under which the laser radiation is focused on the target, the plasma motion, and the curvature of the critical surface. When allowance is made for the first two of these factors, the spectral density of the second-harmonic energy flux, $q_{n'}^{(2)}$, in the direction n' is given by the formula²⁰

$$q_{n'}^{(2)} = \frac{1}{128\pi} \frac{e^2}{m^2 c \omega_0^2} E_p^4(\theta_0, \varphi_0) \left(\frac{\omega_0 L}{c}\right)^2 \sin^2 \theta_0 \Phi^4(\theta_0) \times (3 - 4 \sin^2 \theta_0)^{1/2} \cos \theta_0 \delta(\omega' - 2\omega_0 - 2(k_0 - k_0 n', u)) \times \exp\{-2\tau_1 - \tau_2 - \tau_{\text{eff}}(3 - 4 \sin^2 \theta_0)^{1/2}\}, \quad (1)$$

where $k_0 = \omega_0/c$, u is the velocity of motion of the critical-density surface, φ_0 is the angle between the plane of polarization of the pump wave (k_0, E_0) and the incidence plane (k_0, x), $E_p = E_0 \cos \varphi_0$ is the p component of the electric field, and L is the characteristic scale of the variation of the density in the vicinity of the critical point $x=0$.

In the formula (1)

$$\tau_1 = \nu_{ei}/(v_{ei}L/c) \cos^2 \theta_0, \quad \tau_2 = \frac{2\nu_{ei}L}{c} \left\{ 128 \cos^3 \theta_0 - \left(\frac{3}{4} - \sin^2 \theta_0\right)^{1/2} [147 - 272 \sin^2 \theta_0 + 128 \sin^4 \theta_0] \right\} \frac{1}{15},$$

$\tau_{\text{eff}} = 2\nu_{\text{eff}}L/c$, where the effective collision rate, $\nu_{\text{eff}} = \max\{\nu_{ei}, \omega_0(r_D/L)^{2/3}\}$, is determined either by the electron-ion collision rate, ν_{ei} , in the critical region, or by the export of plasma waves from the resonance region (r_D is the Debye radius of the electron in the critical region). The function $\Phi(\theta_0)$ characterizes the dependence of the linear-conversion factor on the angle, θ_0 , of incidence of the wave on the plasma.⁵ For $u=0$, $\nu_{ei} = \nu_{\text{eff}} = 0$, $\varphi_0 = 0$, and $\theta_0 \ll 1$, the formula (1) corresponds up to a numerical factor of the order of unity with the results of Refs. 4, 9, and 19.

The second-harmonic radiation has the same polarization as the pump wave, and is emitted specularly with respect to the latter wave ($\theta' = \theta_0$, $\varphi' = \varphi_0 + \pi$, where $\cos \theta' = n'_z$, and φ' is the angle between the plane of emission of the harmonic and plane of polarization of the pump wave). According to (1), the second-harmonic radiation frequency

$$\omega_2 = 2\omega_0 - 2(k_0 - k_0 n', u) \quad (2)$$

is shifted relative to the nominal value of $2\omega_0$ in the blue or red direction, depending on whether the critical-density surface moves towards ($u > 0$), or away from ($u < 0$), the beam. The maximum value of the shift,

$$\Delta\omega_2 = \omega_2 - 2\omega_0 = 4\omega_0 u/c, \quad (3)$$

is attained when the pump wave is incident along the direction of divergence of the plasma.

The spectral width, $\delta\omega_2$, at any given moment of time is determined by twice the spectral width of the pump: $\delta\omega_2 = 2\delta\omega_0$. The change in the velocity u during the time of registration of the harmonic, characterized by the

quantity δu , leads to additional broadening of the spectrum when the exposure time is sufficiently long:

$$\delta\omega_2 = 2\delta\omega_0 + 4\omega_0 \delta u/c. \quad (4)$$

The quantity $q_{n'}^{(2)}$, integrated over the angles and frequencies, determines the energy flux in the second harmonic:

$$q_2 = \int d\omega' d\Omega' q_{n'}^{(2)}. \quad (5)$$

The p -component amplitude E_p entering into $q_{n'}^{(2)}$ is determined by the focusing conditions for the heating radiation. In the case most often realized in experiment, when the optical axis of the focusing system is oriented along the normal to the target surface, the incident light beam has a circular cross section, is linearly polarized, and its intensity is uniformly distributed over the cross section:

$$E_p^2(\theta_0, \varphi_0) = \frac{4E_0^2 \cos^2 \varphi_0}{\pi s^2 \cos^2 \theta_0}, \quad 0 < \varphi_0 < 2\pi, \quad 0 < \theta_0 < \theta_m;$$

here $\theta_m = \tan^{-1}(s/2)$ is the maximum angle of convergence of the rays of the heating beam with respect to the optical axis, and is determined by the aperture ratio of the focusing system: $s = D/F$ (D is the diameter of the lens; F its focal length).

For short-focus objective lenses, when $\tan^{-1}(s/2) \gg \sin^{-1}\theta_r$, we obtain from (1) and (5) the expression

$$K_2 = \frac{q_2}{q_0} = 0.15 \frac{q_0}{n_e m c^3 s^4} \left(\frac{\omega_0 L}{c}\right)^{1/2} \exp\left(-3.46 \frac{\nu_{\text{eff}} L}{c} - 2.22 \frac{\nu_{ei} L}{c}\right) \quad (6)$$

[$\sin \theta_r = 0.46(c/\omega_0 L)^{1/3}$ is the optimum—for linear conversion—angle of incidence of the radiation ($\Phi(\theta_r) \approx 1$)].

In the other limiting case of long-focus systems, when $s \ll (c/\omega_0 L)^{1/3}$,

$$K_2 = 0.23 \frac{q_0}{n_e m c^3 s^4} \left(\frac{\omega_0 L}{c}\right)^{1/2} \exp\left(-3.46 \frac{\nu_{\text{eff}} L}{c} - 2.22 \frac{\nu_{ei} L}{c}\right). \quad (7)$$

The maximum value of the conversion factor K_2 is attained in the case when the angle of convergence of the beam is close to the resonance value.

Let us emphasize that the above-presented formulas are valid for a plane plasma layer. They can be used for the computation of the intensity of the harmonic in experiments with picosecond laser pulses. For the interpretation of experiments with nanosecond pulses, it is necessary to take account of the shape of the critical surface (the multidimensionality of the density inhomogeneity) in the case when the radius of curvature, R_c , of the critical surface is comparable to the dimension, d , of the focal spot. For $R_c \lesssim d$, a considerable portion of the incident radiation is refracted in the tenuous regions of the corona before it reaches the critical surface. Therefore, only the rays inclined at an angle of $\theta_0 \sim \theta_r$ to the normal to the critical surface participate in the harmonic generation. Since these rays carry $\sim (R_c \theta_r/d)^2$ of the energy of the laser beam, the coefficient K_2 should, when $R_c \lesssim d$, decrease by a factor of θ_r^{-4} , i.e.,

$$K_2 = \left(\frac{2R_c}{d}\right)^4 \frac{q_0}{n_e m c^3} \left(\frac{\omega_0 L}{c}\right)^{1/2} \frac{1}{s^4} \exp\left(-3.46 \frac{\nu_{\text{eff}} L}{c} - 2.22 \frac{\nu_{ei} L}{c}\right). \quad (8)$$

As will be shown, the use of this formula allows us to obtain satisfactory agreement with the majority of the

available experimental data.

In the case when intense plasma oscillations are excited in the vicinity of the critical surface as a result of the development in the plasma of parametric instabilities, the harmonic arises either as a result of the merging of two plasma oscillations ($l+l \rightarrow t$), or as a result of the merging of a longitudinal oscillation with the pump wave ($l+t \rightarrow t$). For the first process, resonance interaction is possible for Langmuir oscillations with virtually any wave-length. The dimension, Δx_{ll} , of the region of resonance generation turns out in this case to be large: $\Delta x_{ll} \approx 3(k_{st} R_D)^2 L$, where $k_{st} \approx r_D^{-1} \ln^{-1/2} \times (\omega_0/\nu_{ei}) \approx 0.3 r_D^{-1}$ is the maximum wave number of the parametrically excitable Langmuir waves. In the case of the $l+t$ merging, only the long-wave plasma oscillations ($k_l \sim \omega_0/c$) participate in the generation of the $2\omega_0$ harmonic. In this case the dimension, $\Delta x_{lt} \approx (v_{Te}/c)^2 L$, of the region of resonance generation of the harmonic turns out to be significantly less than the quantity Δx_{ll} .

A comparison of the probabilities for these mergings showed that the $l+l$ process governs the harmonic generation if the field intensity, E_1 , of the Langmuir waves is sufficiently high, i.e., if

$$E_1^2 \Delta x_{ll} > E_0^2 \Delta x_{lt}. \quad (9)$$

Taking into account the fact that the energy density of the Langmuir waves parametrically excitable in the critical-density region is either equal to, or greater than, the pump-energy density (see Refs. 21–23), we can conclude that the two-plasmon merging process plays the dominant role. Furthermore, it should be borne in mind that the smallest wave number possible for the Langmuir waves in an inhomogeneous plasma $k_{\min} \sim (r_D^2 L)^{-1/3}$. Therefore, for $k_0 L < c^2/v_{Te}^2$, when $k_{\min} > \omega_0/c$, the $l+l \rightarrow t$ process is generally strongly suppressed.

Under conditions of a small excess over the parametric-instability threshold, the spectral density of the plasmon energy, $W_1(\mathbf{k}, x)$, is anisotropic: the wave vector, \mathbf{k} , of the Langmuir waves is oriented along the pump-polarization vector \mathbf{e}_0 . In this case, using the formulas of Pustovalov and Silin's monograph,²⁴ we obtain the following distribution of the intensity of the harmonic over the directions, \mathbf{n} , of its emission:

$$q_{\mathbf{n}, \omega}^{(2)} = (\mathbf{n} \cdot \mathbf{e}_0)^2 (\mathbf{e} \cdot \mathbf{e}_0)^2 \left(n_x^2 + \frac{\Delta x_{ll}}{3L} \right)^{-1/2} q_2(\omega) e^{-\tau_x}, \quad (10)$$

where $q_2(\omega)$ is the spectral distribution of the harmonic radiation:

$$q_2(\omega) = \frac{6\sqrt{3}}{(2\pi)^3} \frac{\omega_0^4}{n m c^5} \int_0^{\Delta x_{ll}} dx \int dk' W_1(k', x) W_1(\mathbf{k}-\mathbf{k}', x) \delta(\omega - \omega_l(k') - \omega_l(\mathbf{k}-\mathbf{k}')), \quad (11)$$

\mathbf{e} is the polarization vector of the harmonic,

$$\tau_x(\mathbf{n}) = \frac{\nu_{ei} L}{15c} [8(1+3n_x^2)^{3/2} - 3\sqrt{3}|n_x| (5+20n_x^2+24n_x^4)]$$

is the optical thickness of the plasma at the second-harmonic frequency.

For high pump fluxes the plasma turbulence can be considered to be isotropic. In this case, instead of

(10), we have

$$q_{\mathbf{n}, \omega}^{(2)} = \frac{1}{15} \left[n_x^2 + \frac{\Delta x_{ll}}{3L} \right]^{-1/2} q_2(\omega) e^{-\tau_x}. \quad (12)$$

As a result of the refraction of the second-harmonic radiation in the corona, the direction, \mathbf{n} , of its emission does not coincide with the direction, \mathbf{n}' , in which it is registered outside the plasma: $\varphi = \varphi'$, $\sin \theta' = (\sqrt{3}/2) \sin \theta$. The refraction brings about the existence of a limiting angle $\bar{\theta}_m = 65^\circ$ ($\Delta x_{ll}/3L \approx 0.1$). The second harmonic should not register at $\theta' \sim \bar{\theta}_m$. In the case of isotropic turbulence the intensity of the harmonic does not depend on the angle, φ , of its emission relative to the polarization plane of the pump wave.

According to the formula (11), the second-harmonic frequency is determined by the sum of the frequencies of the merging Langmuir waves: $\omega_2 \approx 2\omega_l(k_l)$. The parametric turbulence in the critical-density region arises as a result of the decay of the pump wave into longitudinal Langmuir and low-frequency oscillations. Therefore, the frequencies of the Langmuir waves, $\omega_l(k_l) = \omega_0 - \omega(k_l)$, are lower than the value of ω_0 , and there occurs a red shift of the harmonic frequency relative to the nominal value,

$$\Delta \omega_2 = -2\omega(k_l), \quad (13)$$

which is determined by the frequency of the low-frequency waves that are parametrically excited during the instability. Under conditions of weak parametric coupling of the waves, i.e., for

$$q < q_m = 16(\omega_{Li}/\omega_{Le}) k_{st} r_D c n_e T_e \quad (14)$$

(q is the flux density of the pump in the critical region), the quantity ω is equal to the frequency of the ion-acoustic waves: $\omega = \omega_s = \omega_{Li} k_l r_D$ (ω_{Li} is the ion Langmuir frequency). For $q > q_m$, the frequency $\omega = \omega_s^{2/3} \omega_0^{1/3} (q/c n_e T_e)^{1/3}$ grows in proportion to $q^{1/3}$.

On account of the dependence of k_l on the coordinate x , different points of the density profile give different harmonic-frequency shifts. The maximum shift in frequency occurs in the merging of short-wave Langmuir waves (i.e., waves with $k_l \sim k_{st}$), which are the waves that are most efficiently excited.²¹

The effect of the divergence of the plasma and the motion of the critical surface on the shift and shape of the harmonic line in the case of parametric generation turns out to be negligible.

The broadening of the spectrum of the harmonic on the red side from the value $\Delta \omega_2 = 2\omega_s(k_{st})$ is connected with the processes of nonlinear transfer of the energy of the oscillations into the region of lower frequencies.^{22, 23} The broadening on the blue side is explained by the excitation during the parametric instability of the oscillations not only with frequencies lower than ω_0 , but also with a few higher frequencies. The blue shift should be of the order of the increment of the parametric instability, and is therefore always less than the red shift.

The spectral width (13) is significantly greater than (4). Therefore, the parametric generation should lead to a wide "pedestal" with narrow line due to the linear

conversion process in its background.

Under the conditions of a collision-governed regime of parametric-turbulence saturation, i.e., for $q < 10^{14} AZ^{1/2} \lambda_0^{-7/2} T_e^{-5/4} \text{ W/cm}^2$ (T_e is in keV and λ_0 is in μ),²³ we can derive an explicit expression for K_2 , using, for example, the parametric-turbulence level and spectrum found in Refs. 21–23:

$$K_2 = 4 \cdot 10^{-19} Z^{-1} T_e^3 L q_0 \lambda_0^3 \exp(-2.2 \nu_e L / c). \quad (15)$$

It can be seen that K_2 grows in proportion to the cube of the temperature and to the product $q_0 \lambda_0^3$, i.e., to the square of the amplitude of the electron oscillations in the field of the light wave.

At large values of the energy-flux density, when the parametric turbulence has a collisionless character, the formula (15) is no longer applicable. Nevertheless, we can give the following estimate for the magnitude of the energy flux in the second harmonic (due to the $l+l$ process):

$$q_2 = 10^2 \frac{L}{\lambda_0} \left(\frac{v_{Te}}{c} \right)^5 \left(\frac{E_L^2}{8\pi n_e T_e} \right)^2 n_e c T_e.$$

This formula can be used to estimate the turbulence level in the vicinity of the critical point from experimental measurements of the second-harmonic intensity.

§2. EXPERIMENTAL INVESTIGATION ON THE "KAL'MAR" FACILITY OF SECOND-HARMONIC GENERATION DURING THE IRRADIATION OF SHELL TARGETS

With the object of justifying the above-exposed theoretical model and verifying the consequences following from it, we performed on the "Kal'mar" nine-channel neodymium-glass laser facility²⁵ experimental investigations of the distinctive features of second-harmonic generation during the irradiation of gas-filled SiO_2 -glass microspheres.

The observation was conducted in several recording channels (Fig. 1): backwards into the apertures of the

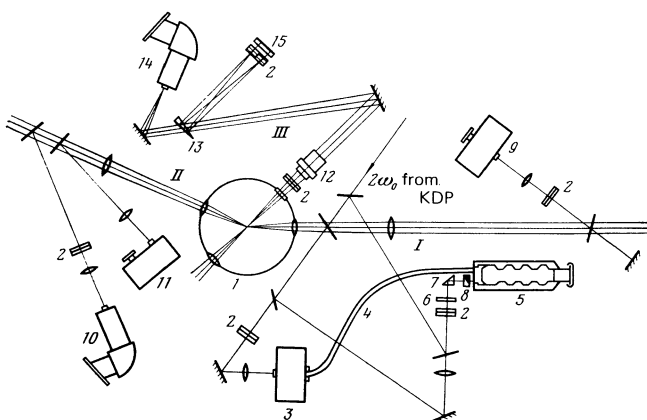


FIG. 1. Schematic representation of the arrangement of the spectral diagnostic apparatus: I), II), III), recording channels, 1) vacuum chamber, 2) light filters, 3) MDR-2 monochromator, 4) flexible light conductor, 5) photoelectric recorder, 6) scatterer, 7) prism, 8) step attenuator, 9) MDR-2 monochromator, 10) ISP-51 spectrograph, 11) VMS-1 spectrograph, 12) objective lens, 13) wedge, 14) ISP-51 spectrograph, 15) film holder.

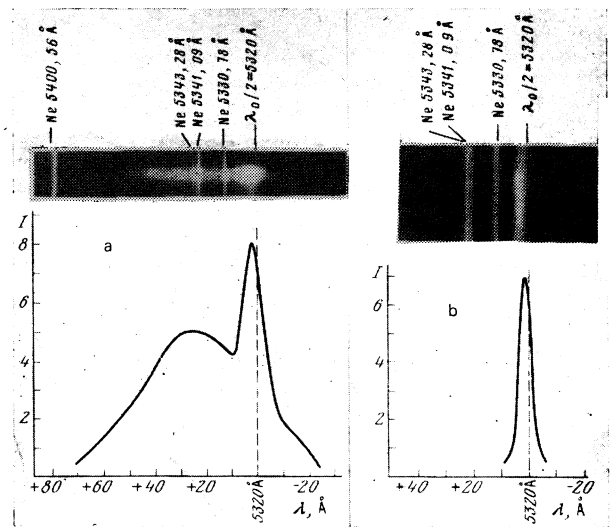


FIG. 2. Second-harmonic radiation spectrograms integrated over time and the target surface: a) $q_0 \approx 10^{14} \text{ W/cm}^2$, b) $q_0 \approx 10^{13} \text{ W/cm}^2$.

focusing systems for the heating beams (I, II) and through the diagnostic window of the vacuum chamber (III). In the latter case the use of a long-focus ($F \approx 300 \text{ cm}$) objective lens, we, which threw the image of the target on the slit of the prism spectrograph 14, allowed us to achieve a spatial resolution with respect to the object of $\approx 15 \mu$, and also photograph the plasma in the $2\omega_0$ -harmonic self-radiation (13, 15). To ensure time resolution, we used a monochromator, 3, in conjunction with a photoelectric recorder, 5, operating in the slit-scanning regime with a time resolution $\leq 0.1 \text{ nsec}$. The spectrally decomposed radiation was transmitted by the light conductor 4 to the photorecorder's slit, which was located along the dispersion direction of the monochromator. The spectral resolution of the recording system was $\approx 1.5 \text{ \AA}$.

In Fig. 2a we show a time-integrated spectrogram of the second harmonic, recorded at an energy-flux density on the target of $q_0 \approx 10^{14} \text{ W/cm}^2$. A two-component structure of the spectrum can clearly be seen. In conformity with the model, the narrow component is due to harmonic generation by the p component of the pump field. In fact, this line was recorded at $q_0 \approx 10^{13} \text{ W/cm}^2$, which is less than the parametric-instability thresholds. The spectrum of the harmonic (see Fig. 2b) consists of one peak having a width not exceeding the width of the spectrum of the pump, and shifted by an amount $\approx 1.7 \text{ \AA}$ into the red region. For $q_0 \approx 10^{14} \text{ W/cm}^2$ (Fig. 2a), the spectral width of the narrow line also corresponds with the formula (4), and is determined by the spectral width of the pump. The "red" shift of the narrow component in Fig. 2a ($\Delta\lambda \approx 2.5 \text{ \AA}$) gives, according to (3), the velocity of the motion of the critical surface into the target to be $u \approx 7.3 \times 10^6 \text{ cm/sec}$. To confirm the connection between the shift of the narrow component and the Doppler effect, we performed, for the first time, supplementary experiments.

1. A spectrogram of the harmonic was obtained with spatial resolution with respect to the target. As can be seen from Fig. 3, the shift of the narrow component is

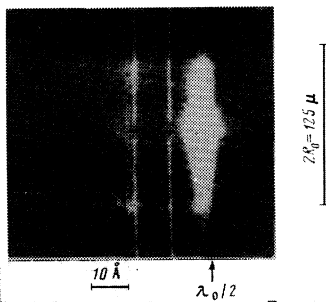


FIG. 3. Spectrogram of the second-harmonic radiation, recorded with spatial resolution ($q_0 \approx 10^{14}$ W/cm²), for a glass shell target. The gap between the reference spectral lines corresponds to the center of the target image.

not the same for different regions. To wit: the shift is greatest near the gap between the reference spectral lines, which passes through the center of the target (in Fig. 3 the maximum shift is ≈ 1.5 Å), and close to zero in the boundary regions, which corroborates the theoretical model. Indeed, in the case of spherically symmetric scattering of the plasma, the component of the velocity of the critical-density surface in the direction of observation is maximal for the regions of the corona that correspond to the central part of its image, and equal to zero for the boundary region.

2. To reconstruct the evolution of the velocity of the critical surface, we recorded the spectrum of the harmonic with a time resolution of 0.1 nsec. In Fig. 4b we show a typical time scan of the spectrum of the $2\omega_0$ harmonic, obtained with the aid of a spectral instrument and a photoelectric recorder (streak photograph) and Fig. 5 shows the spectral distributions obtained in the processing of the time scan. The wavelength of the narrow component is observed to increase in time. For $t < 0.5$ nsec the shift of the narrow component is "blue." In particular, at the moment $t \approx 0.1$ nsec the shift is $\Delta\lambda \approx 2$ Å, which corresponds to motion toward the beam with a velocity of $u \approx 6 \times 10^6$ cm/sec. At $t > 0.5$ nsec there arises a "red" shift that increases in time. To

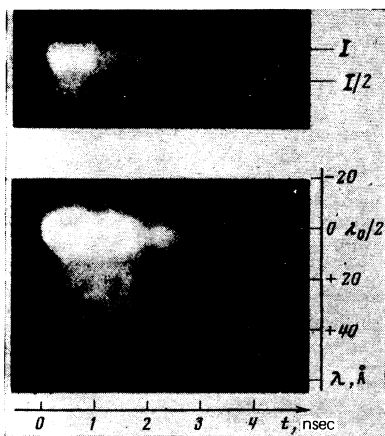


FIG. 4. Time scans of: a) the intensity of the heating radiation ω_0 , b) the spectrum of the $2\omega_0$ -harmonic radiation for a glass shell target of diameter $2R_0 = 163$ μ and wall thickness $\Delta R \approx 4.6$ μ ; $q_0 \approx 10^{14}$ W/cm².

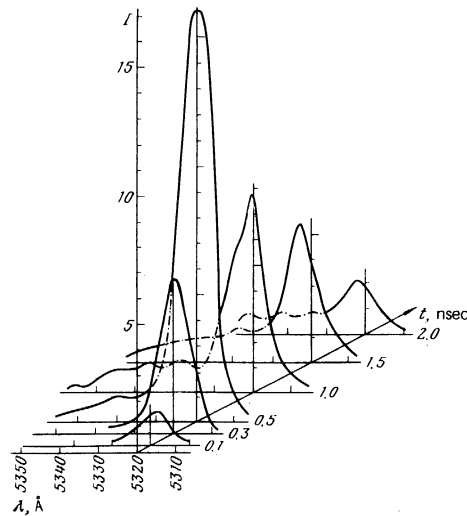


FIG. 5. Spectral distributions of the second-harmonic radiation at different moments of time for the photogram shown in Fig. 4b.

the maximum "red" shift $\Delta\lambda \approx 2$ Å at the moment $t \approx 2.0$ nsec corresponds a target-compression rate of $u \approx 6 \times 10^6$ cm/sec.

3. Such a picture of the motion of the critical surface was corroborated by its R - t plots, obtained by time scanning the image on the photoelectric recorder of the plasma in the second-harmonic self-radiation.²⁶ This is another corroboration of the possibility of using the time scan of the spectrum of the harmonic to study the dynamics of shell compression.

4. It can be seen from Fig. 5 that, for thin-walled shells, the most intense generation of the narrow line in the $2\omega_0$ spectrum occurs during the motion of the critical-density region toward the center of the target. Therefore, even the time-integrated spectrograms carry information about the rate of collapse of the shell. In this case, as the shell thickness is increased, the "red" shift of the narrow component should decrease as a result of the decrease in the collapse rate. This effect was experimentally observed (see Fig. 6). The decrease of the mean rate of collapse with increasing shell thickness is also confirmed by hydrodynamic calculations.²⁷

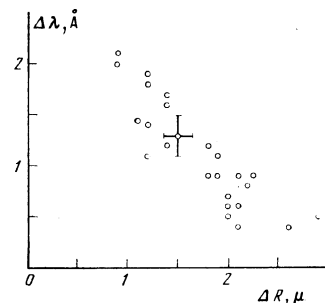


FIG. 6. Dependence of the magnitude of the time-integrated shift of the principal second-harmonic component (relative to the exact value $\lambda_0/2$) on the thickness of the wall of the glass shell targets for a laser-radiation flux density of $q_0 \approx 10^{14}$ W/cm².

The spectrum of the second harmonic in Fig. 2a differs from the case of low fluxes (Fig. 2b) in that there is observed, besides the principal (narrow) component, a pedestal, shifted in the "red" direction, and having a width of up to 100 \AA at the 0.1-intensity level. The pedestal has, as a rule, the shape of a broad satellite component whose peak is shifted in the direction of longer wavelengths by $20\text{--}30 \text{ \AA}$. The ratio of the intensities of the satellite and principal components varied from flare to flare within the limits 0.1–0.6. In some of the spectrograms we found the spectrum of the satellite component to be modulated with peak spacings of $3\text{--}10 \text{ \AA}$.

The existence of a pedestal at $q_0 \approx 10^{14} \text{ W/cm}^2$ indicates that the threshold for parametric instability had been exceeded. For the value, $T_e \approx 0.6 \text{ keV}$, of the electron temperature that obtained in the experiment (it was measured from the spectrum of the $\frac{3}{2}\omega_0$ harmonic²⁸) and the corresponding mean ion charge $Z \approx 9$, we find, according to Ref. 6 that (L is in μ)

$$q_{0 \text{ thr}} \approx 1.6 \cdot 10^{13} \exp(L/15) \quad (16)$$

[W/cm²].

The absence of the pedestal at $q_0 \approx 10^{13} \text{ W/cm}^2$ and its presence at $q_0 \approx 10^{14} \text{ W/cm}^2$ allow us to give with the aid of the formula (16) an upper limit for the characteristic inhomogeneity dimension: $L < 25 \mu$. This estimate agrees well with the experimental value of $L \approx 20 \mu$, obtained from measurements of the distance between the generation regions for the $2\omega_0$ and $\frac{3}{2}\omega_0$ harmonics,²⁹ and with the results of numerical hydrodynamic calculations²⁷ performed for conditions similar to ours. The "red" shift, $\Delta\lambda_p \approx 20\text{--}30 \text{ \AA}$, of the peak of the pedestal is in accord with the formula (13) ($\Delta\lambda_p = 25 \text{ \AA}$) if as the frequency ω , we substitute the frequency, ω_s , of the ion sound with wave number $k_i \sim k_{st}$. This is valid under the conditions, (14), of weak parametric coupling of the waves, conditions which were fulfilled in our experiment, since $q_m \approx 2 \times 10^{14} \text{ W/cm}^2$.

A comparative analysis of the photographs of the plasma radiation in the $2\omega_0$ region and the spectrograms recorded with spatial resolution showed that the broad component is emitted predominantly by the regions corresponding to the boundary regions of the image (see Fig. 3). This fact finds its explanation within the framework of our model under the assumption that the directivity pattern for the harmonic emission is isotropic, which indicates the isotropy of the parametric turbulence.

On the other hand, the "bright spots" recorded on the photographs of the plasma in the central part of the image of the corona³⁰ are connected with the radiation of the narrow component. Their shape varies from flare to flare even in the case of a highly uniform irradiation of the target. Such an image structure is apparently connected with the spatial regions corresponding to the optimum angle, $\theta_0 \approx \theta_r$, of incidence of the radiation of the various laser beams on the plasma.

The geometry of our experiment did not allow us to carry out a direct measurement of the total coefficient of conversion of the heating radiation into the second

harmonic. Under the assumption, however, that the resulting directivity pattern for the harmonic emission is isotropic, we can estimate the magnitude of the conversion factor to be $K_2 \approx 10^{-6}\text{--}10^{-7}$. The local conversion factor attained a value of $K_2 \approx 10^{-5}$ in the regions of maximum radiant emittance. For the typical parameters of the radiation and the plasma that obtained in the experiments ($q_0 \approx 10^{14} \text{ W/cm}^2$, $L \approx 20 \mu$, $T_e \approx 0.6 \text{ keV}$, $Z \approx 9$, $A = 20$, $d/R_c \approx 3$), we find, using the formulas (8) and (15), that the coefficient of conversion into the principal component is $K_2 = 6 \times 10^{-6}$, while the coefficient of conversion into the satellite component is $K_2 \approx 3 \times 10^{-6}$.

Thus, the performed analysis allows to conclude that our model of harmonic generation is in satisfactory agreement with the experimental data obtained on the "Kal'mar" facility.

§3. ANALYSIS OF THE EXPERIMENTS ON SECOND-HARMONIC GENERATION IN A LASER PLASMA

We have at present a large quantity of experimental data on second-harmonic generation in a laser plasma. At first glance, some of these data even contradict each other. However, as will be shown, virtually all of them find their interpretation within the framework of our model. We shall discuss the experiments performed with the aid of neodymium lasers.

The angular distribution of the intensity of the $2\omega_0$ radiation has been studied largely at relatively low pump-flux densities ($\leq 10^{14} \text{ W/cm}^2$), where the instability thresholds could not have been appreciably exceeded. Under these conditions, we cannot expect the parametric processes to play the dominant role in second-harmonic generation, and the laws governing the generation are largely determined by the linear-conversion process. This assertion is corroborated by the experiments described in Refs. 31–33, in which the harmonic is studied mainly in the specular direction with respect to the heating beam.

The most complete information we have is about the spectra of the second harmonic. The experiments were performed in a broad range of flux densities: $10^{12}\text{--}10^{16} \text{ W/cm}^2$. The principal results of the time-integrated measurements made with the use of a spectrally narrow ($\sim 1\text{--}10 \text{ \AA}$) pump are shown in Fig. 7, where we can clearly see two typical harmonic spectra, having the shape of either a relatively narrow line of width $\sim 2\text{--}20 \text{ \AA}$ [the curves a), b), g), and h)], or a narrow line with a broad ($\sim 100\text{--}400 \text{ \AA}$) pedestal [the curves c), d), e), and f)]. It is characteristic that the narrow harmonic line is observed at low ($\leq 10^{13} \text{ W/cm}^2$) and, conversely, high ($\geq 10^{15} \text{ W/cm}^2$) flux densities. The pedestal, on the other hand, appears in the moderate flux range ($\sim 10^{14}\text{--}10^{15} \text{ W/cm}^2$).

The above-noted features of the shape of the harmonic spectra can be understood on the basis of the above-exposed model if we take into account the fact that the linear-conversion process leads to the appearance of a narrow line, while the parametric turbulence leads to a broad spectral distribution, i.e., to a pedestal. Therefore, there should be no pedestal in the case when

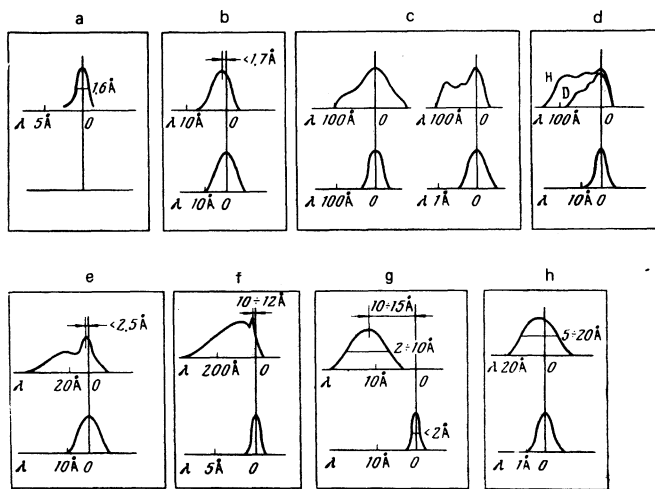


FIG. 7. Spectra of the second-harmonic (upper curves) and the heating radiation ω_0 (lower curves), obtained in different experiments on the action on a target of the radiation of a ruby (a— $q_0 = 5 \times 10^{12}$ W/cm² (Ref. 34)) and a neodymium (b— $q_0 = 10^{13}$ W/cm² (Ref. 35)), c— $q_0 = 5 \times 10^{13}$ W/cm² (Refs. 7 and 8), d— $q_0 = 3 \times 10^{13} - 3 \times 10^{14}$ W/cm² (Ref. 36), e— $q_0 = 10^{14}$ W/cm² (Refs. 35 and 37), f— $q_0 = 10^{15} - 10^{16}$ W/cm² (Ref. 12), g— $q_0 = 3 \times 10^{15} - 2 \times 10^{16}$ W/cm² (Ref. 38), h— $q_0 > 10^{16}$ W/cm² (Ref. 39) laser.

the development of the parametric instabilities is inhibited. This should, in the first place, occur when the threshold instabilities have not been exceeded. Secondly, the twisting of the density profile at high fluxes also results in the suppression of the instabilities and, consequently, in the nonappearance of the pedestal. The most severe twisting of the profile occurs when the light pressure is comparable to the gas-kinetic pressure of the plasma. The spectra a) and b) in Fig. 7 correspond to the case when the parametric-instability thresholds have not been exceeded. The spectra g) and h), on the other hand, can be related with the twisting of the density profile.

Notice that the narrow line in each of the spectra shown in Fig. 7 is shifted by 1–15 Å in the "red" direction. Consequently, the most intense emission of the $2\omega_0$ line occurs during the motion of the critical-density surface into the target. According to (3), the quantity u varied in the experiments from 3×10^6 to 4×10^7 cm/sec.

The manifestation of the two $2\omega_0$ -harmonic generation mechanisms is also indicated by the experiments in which the polarization of the harmonic was studied. In particular, the existence of the two mechanisms explains two seemingly mutually exclusive results: the retention of the polarization of the pump by the harmonic⁴⁰ and the absence of harmonic polarization.⁸ The first result⁴⁰ was obtained in a procedure in which the radiation propagating backwards into the focusing lens was recorded, while the second result⁸ was obtained in the registration of the radiation propagating at an angle of 45° to the heating beam. In either case the irradiating beam was normal to the target surface. The linear conversion process preserves the polarization of the pump, and makes the dominant contribution

to the generation of the harmonic emitted in the specular direction. Therefore, the preservation of the polarization in the experiment described in Ref. 40 is due to the linear conversion mechanism, since the angles of specular scattering did not exceed the angular aperture of the focusing lens. On the other hand, we cannot, for a large angle of observation^{7,8} exceeding the angles of specular scattering, count on the linear-conversion mechanism's playing a significant role and, consequently, on the preservation of the pump polarization. The depolarization of the $2\omega_0$ radiation in this case is due to the dominant role played by the parametric instabilities in the harmonic generation. Let us emphasize that this assumption is in accord with the observed spectrum (see Fig. 7c), which exhibits a well pronounced pedestal.

Experimental investigations of the dependence of the harmonic intensity on the energy-flux density of the pump at low fluxes $q_0 \lesssim 10^{14}$ W/cm² have been performed by a number of experimenters.^{3,17,33,41,42} It was observed that the intensity of the harmonic grows in proportion to q_0^α , where $\alpha \leq 2$. At such fluxes q_0 , the harmonic generation is due largely to the linear conversion mechanism, and, in accordance with the formula (1), the intensity of the harmonic should be proportional to q_0^2 (i.e., $\alpha = 2$). However, in the experiments described in Refs. 41–43, α turns out to be slightly less than two. This, in our opinion, is explained by the decrease with increasing pump flux of the characteristic dimension, L , of the density inhomogeneity. At the flux densities under discussion ($\lesssim 10^{14}$ W/cm²), such a decrease of L cannot be related with strictional forces, and is, apparently, due to the variation of the hydrodynamic conditions for the scattering of the plasma as the flux of the heating radiation increases. On the other hand, the observation in the experiment described in Ref. 12 of the second-harmonic intensity dependence $\propto q_0^\alpha$, where $\alpha > 2.5$, for $q_0 \sim 10^{15}$ W/cm² can be understood if we take account of the fact that a significant contribution can be made to the harmonic generation by the parametric processes (this is indicated by the spectral distribution of the harmonic; see Fig. 7f). In accordance with the formula (15), the increase in the exponent α in comparison with $\alpha = 2$ in this case can be related with the dependence of the electron temperature, T_e , of the plasma on the pump-flux density. Indeed, the critical dependence on T_e of the second-harmonic intensity ($\propto T_e^3 q_0^2$) can lead to a sharp change in the growth of the energy of the harmonic in comparison with the q_0^2 dependence even when the temperature increases slowly with increasing q_0 .

Let us note that a comparison of the results of the theory and experiment yields a satisfactory agreement for the magnitude of the second-harmonic intensity. Let us illustrate this, using the specific example of, for example, Ref. 33. Let us assume as a basis the following experimental data: $q_0 \approx 4 \times 10^{14}$ W/cm², $L \approx 1 \mu$, $T_e \approx 0.5$ keV, $Z = 6$, $\lambda_0 \approx 1 \mu$, $s \approx 1$, $K_2 \approx 10^{-5}$. Bearing in mind the smallness of the characteristic dimension of the density inhomogeneity ($\sim 1 \mu$), we can conclude that the parametric instabilities make a small contribution to the second-harmonic intensity. Then,

using the formula (6), we obtain for the conversion factor the value $K_2 \approx 10^{-5}$, which is in good agreement with the experimentally obtained estimate.

CONCLUSION

The above-performed analysis allows us to conclude that the theoretical model, formulated in §1, of second-harmonic generation in a laser plasma has been experimentally confirmed. This opens up the possibility of using the harmonic for determining such parameters of the corona as the dimension of the density inhomogeneity and the velocity of the motion of the critical surface. Finding from the spectral measurements of the $\frac{3}{2}\omega_0$ harmonic the temperature of the plasma,²⁸ we can determine virtually all the laser-plasma-corona parameters of interest to us with a high time and spatial resolution.

Notice that the diagnostic methods proposed by us can be used not only for the investigation of a plasma heated by a laser, but also in plasma facilities of other types (see Ref. 44). Thus, for example, the use of a relatively low-power probing laser ($q_0 \sim 10^{13}$ W/cm²) in experiments on plasma heating by electron and ion beams will allow the determination of the plasma parameters in a region where the density is close to the critical density for the radiation used.

- ¹A. Caruso, A. de Angeles, G. Gatti, R. Gratton, and S. Martellucci, *Phys. Lett.* **33A**, 29 (1970).
- ²M. Decroisette, B. Meyer, and G. Piar, *J. Phys.* **C32**, 56, 119 (1971).
- ³A. A. Rupasov, V. P. Tsapenko, and A. S. Shikanov, *Preprint Fiz. Inst. Akad. Nauk SSSR*, No. 94 (1972).
- ⁴N. S. Erokhin, V. E. Zakharov, and S. S. Moiseev, *Zh. Eksp. Teor. Fiz.* **56**, 177 (1969) [*Sov. Phys. JETP* **29**, 101 (1969)].
- ⁵N. G. Denisov, *Zh. Eksp. Teor. Fiz.* **31**, 609 (1956) [*Sov. Phys. JETP* **4**, 544 (1957)].
- ⁶V. P. Silin, *Parametricheskoe vozdeistvie izlucheniya bol'shoi moshchnosti na plazmu* (Parametric Effect of High-Power Radiation on a Plasma), Nauka, Moscow, 1973.
- ⁷M. Decroisette, B. Meyer, and Y. Vitel, *Phys. Lett.* **45A**, 443 (1973).
- ⁸J. L. Bobin, M. Decroisette, B. Meyer, and V. Vitel, *Phys. Rev. Lett.* **30**, 594 (1973).
- ⁹A. V. Vinogradov and V. V. Pustovalov, *Zh. Eksp. Teor. Fiz.* **63**, 940 (1972) [*Sov. Phys. JETP* **36**, 492 (1973)].
- ¹⁰V. V. Pustovalov, V. P. Silin, A. N. Starodub, and V. T. Tikhonchuk, *Nelineinaya parametricheskaya generatsiya moshchnogo izlucheniya v plazme. Doklad na II Mezhdunarodnoi konferentsii po teorii plazmy* (Nonlinear Parametric Generation of High-Power Radiation in a Plasma. Report Presented at the Second Intern. Conf. on Plasma Theory), Kiev, 1974.
- ¹¹A. Saleres, M. Decroisette, and C. Patou, *Opt. Commun.* **13**, 321 (1975).
- ¹²A. A. Gorokhov, V. D. Dyatlov, R. N. Medvedev, A. D. Starikov, and A. G. Tuzov, *Pis'ma Zh. Eksp. Teor. Fiz.* **21**, 111 (1975) [*JETP Lett.* **21**, 49 (1975)].
- ¹³O. N. Krokhin, V. V. Pustovalov, A. A. Rupasov, V. P. Silin, G. V. Sklizkov, A. N. Starodub, V. T. Tikhonchuk, and A. S. Shikanov, *Pis'ma Zh. Eksp. Teor. Fiz.* **22**, 47 (1975) [*JETP Lett.* **22**, 21 (1975)].
- ¹⁴E. Fabre, C. Garban, C. Popovics, A. Poqueresse, C. Stenz, and J. Virmont, *Opt. Commun.* **18**, 218 (1976).
- ¹⁵V. Yu. Bychenkov, V. P. Silin, and V. T. Tikhonchuk, *Fiz. Plazmy* **3**, 1314 (1977) [*Sov. J. Plasma Phys.* **3**, 730 (1977)].
- ¹⁶E. Fabre, C. Garban, C. P. Popovics, A. Poqueresse, C. Stenz, and J. Virmont, *Proc. Sixth Intern. Conf. on Plasma Physics and Controlled Nuclear Fusion Research*, Berchtesgaden, 1976.
- ¹⁷J. Mizui, H. Kang, N. Yamaguchi, T. Sasaki, K. Yoshida, T. Yamanaka, and C. Yamanaka, *J. Phys. Soc. Jpn.* **41**, 1334 (1976).
- ¹⁸V. Yu. Bychenkov, Yu. A. Zakharenkov, O. N. Krokhin, A. A. Rupasov, V. P. Silin, G. V. Sklizkov, A. N. Starodub, V. T. Tikhonchuk, and A. S. Shikanov, *Pis'ma Zh. Eksp. Teor. Fiz.* **26**, 500 (1977) [*JETP Lett.* **26**, 364 (1977)].
- ¹⁹N. S. Erokhin, S. S. Moiseev, and V. V. Mukhin, *Nucl. Fusion* **14**, 333 (1974).
- ²⁰A. B. Vladimirovskii, V. P. Silin, and A. N. Starodub, *Kratk. Soobshch. Fiz.* **12**, 34 (1978).
- ²¹V. P. Silin, *J. Phys. (Paris) coll. C6* **38**, Suppl. No. 12, 153 (1977).
- ²²V. Yu. Bychenkov, V. P. Silin, and V. T. Tikhonchuk, *Pis'ma Zh. Eksp. Teor. Fiz.* **26**, 309 (1977) [*JETP Lett.* **26**, 197 (1977)].
- ²³V. P. Silin and V. T. Tikhonchuk, *Pis'ma Zh. Eksp. Teor. Fiz.* **27**, 504 (1978) [*JETP Lett.* **27**, 475 (1978)].
- ²⁴V. V. Pustovalov and V. P. Silin, *Tr. Fiz. Inst. Akad. Nauk SSSR* **61**, 42 (1972).
- ²⁵Yu. V. Afanas'ev, N. G. Basov, O. N. Krokhin, V. V. Pustovalov, V. P. Silin, G. V. Sklizkov, V. T. Tikhonchuk, and A. S. Shikanov, *Vzaimodeistvie moshchnogo lazernogo izlucheniya s plazmoi. Itogi nauki i tekhniki, ser. Radiotekhnika* (Interaction of High-Power Laser Radiation with a Plasma: Results of Science and Technology, Ser. Radio Engineering), Vol. 17, izd. BINITI, Moscow, 1978.
- ²⁶N. G. Basov, A. A. Erokhin, Yu. A. Zakharenkov, N. N. Zorev, A. A. Kologrivov, O. N. Krokhin, A. A. Rupasov, G. V. Sklizkov, and A. S. Shikanov, *Pis'ma Zh. Eksp. Teor. Fiz.* **26**, 581 (1977) [*JETP Lett.* **26**, 433 (1977)].
- ²⁷N. G. Basov, P. P. Volosevich, E. G. Gamalii, S. Yu. Gus'kov, Yu. A. Zakharenkov, O. N. Krokhin, V. B. Rozanov, G. V. Sklizkov, and A. S. Shikanov, *Pis'ma Zh. Eksp. Teor. Fiz.* **28**, 135 (1978) [*JETP Lett.* **28**, 125 (1978)].
- ²⁸A. I. Avrov, V. Yu. Bychenkov, O. N. Krokhin, V. V. Pustovalov, A. A. Rupasov, V. P. Silin, G. V. Sklizkov, V. T. Tikhonchuk, and A. S. Shikanov, *Pis'ma Zh. Eksp. Teor. Fiz.* **24**, 293 (1976) [*JETP Lett.* **24**, 262 (1976)]. *Zh. Eksp. Teor. Fiz.* **72**, 970 (1977) [*Sov. Phys. JETP* **45**, 507 (1977)].
- ²⁹O. N. Krokhin, A. A. Rupasov, G. V. Sklizkov, and A. S. Shikanov, *Doklad na II Vsesoyuznom soveshchani po diagnostike vysokotemperaturnoi plazmy* (Report Presented at the Second All-Union Conf. on High-Temperature-Plasma Diagnostics), Khar'kov, 1977.
- ³⁰N. E. Andreev, Yu. A. Zakharenkov, N. N. Zorev, V. T. Tikhonchuk, and A. S. Shikanov, *Zh. Eksp. Teor. Fiz.* **76**, 976 (1979) [*Sov. Phys. JETP* **49**, 492 (1979)].
- ³¹N. G. Basov, O. N. Krokhin, V. V. Pustovalov, A. A. Rupasov, V. P. Silin, G. V. Sklizkov, V. T. Tikhonchuk, and A. S. Shikanov, *Preprint Fiz. Inst. Akad. Nauk SSSR*, No. 17 (1974).
- ³²V. V. Aleksnadrov, M. V. Brenner, V. D. Vikharev, V. P. Zotov, N. G. Koval'skii, M. I. Pergament, and V. N. Yufa, *Preprint Inst. At. Energ.*, No. 2852 (1977).
- ³³E. Eidmann and R. Sigel, *Phys. Rev. Lett.* **34**, 799 (1975).
- ³⁴E. Jannitti, A. M. Malvezzi, and G. Tondello, *J. Appl. Phys.* **46**, 3096 (1975).
- ³⁵N. G. Basov, Yu. A. Zakharenkov, N. N. Zorev, A. A. Kologrivov, O. N. Krokhin, A. A. Rupasov, G. V. Sklizkov, and A. S. Shikanov, *Zh. Eksp. Teor. Fiz.* **71**, 1788 (1976) [*Sov. Phys. JETP* **44**, 938 (1976)]. N. G. Basov, A. A. Kologrivov, O. N. Krokhin, A. A. Rupasov, A. S. Shikanov, G. V. Sklizkov, Yu. A. Zakharenkov, and N. N. Zorev, *Proc. Thirty-Sixth Nobel Symposium on Nonlinear Effects in Plasmas*, Sweden, 1976, p. 47.

- ³⁶C. Yamanaka, T. Yamanaka, T. Sasaki, J. Mizui, and H. B. Kang, *Phys. Rev. Lett.* **32**, 1038 (1974).
- ³⁷N. G. Basov, A. A. Kologrivov, O. N. Krokhin, A. A. Rupasov, A. S. Shikanov, G. V. Sklizkov, Yu. A. Zakharenkov, and N. N. Zorev, *Laser Interaction and Related Plasma Phenomena*, Vol. 4A, Plenum Press, 1977, p. 479.
- ³⁸J. Soures, L. M. Goldman, and M. Lubin, *Nucl. Fusion* **13**, 829 (1973).
- ³⁹P. Lee, D. V. Giovanielli, R. P. Godwin, and G. H. McCall, *Appl. Phys. Lett.* **24**, 406 (1974).
- ⁴⁰C. Yamanaka, T. Yamanaka, H. B. Kang, M. Waki, and K. Shimamura, *Annu. Rev. Instrum. Plasma Phys.*, April 1972-March 1973, Nagoya University, p. 110.
- ⁴¹A. A. Rupasov, G. V. Sklizkov, V. P. Tsapenko, and A. S. Shikanov, *Zh. Eksp. Teor. Fiz.* **65**, 1898 (1973) [*Sov. Phys. JETP* **38**, 948 (1974)].
- ⁴²V. V. Aleksandrov, S. I. Anisimov, M. V. Brenner, E. P. Velikhov, V. D. Vikharev, V. P. Zotov, V. G. Koval'skii, M. I. Pergament, and A. A. Yaroslavskii, *Zh. Eksp. Teor. Fiz.* **71**, 1826 (1976) [*Sov. Phys. JETP* **44**, 958 (1976)].
- ⁴³N. G. Basov, O. N. Krokhin, V. V. Pustovalov, A. A. Rupasov, V. P. Silin, G. V. Sklizkov, V. T. Tikhonchuk, and A. S. Shikanov, *Zh. Eksp. Teor. Fiz.* **67**, 118 (1974) [*Sov. Phys. JETP* **40**, 61 (1975)].
- ⁴⁴A. S. Shikanov, *Tr. Fiz. Inst. Akad. Nauk SSSR*, Vol. 103, Nauka, 1978, p. 164.

Translated by A. K. Agyei

Kinetic equation for a system of parametrically excited spin waves

I. A. Vinikovetskiĭ, A. M. Frishman, and V. M. Tsukernik

Physicotechnical Institute of Low Temperatures, Academy of Sciences of the Ukrainian SSR
(Submitted 19 July 1978; resubmitted 28 December 1978)
Zh. Eksp. Teor. Fiz. **76**, 2110-2125 (June 1979)

Kinetic equations describing the magnon system of a parametrically excited ferromagnet are derived. The coherent-state representation is used to find the explicit form of the collision integrals. The stationary distribution is found with allowance for the exchange interactions. It is shown that such a distribution is stable with respect to weak relativistic interactions. The problem of pump-field absorption is investigated. It is shown that the absorbed power is dependent only on the interactions that do not conserve the magnon number.

PACS numbers: 75.30.Ds

1. INTRODUCTION

The macroscopic characteristics of a parametrically excited ferroelectric are determined by the pair correlators, $n_k = \langle a_k + a_k^\dagger \rangle$ and $\sigma_k = \langle a_k a_{-k} \rangle$, of the magnon operators. The temporal evolution of the quantities n_k and σ_k is described by kinetic-type equations containing a dynamical part and a collision-integral analog. The aim of the present paper is to find the explicit form of these integrals, something which has not been done before. Further, we investigate the steady-state distribution of the magnons, and look into the problem of energy absorption for such a distribution.

As is well known, by parametric excitation we mean the situation in which, in a trans-threshold pump field, the magnon system is unstable in some region of k space. This leads to the exponential growth of the correlators n_k and σ_k in time. We assume that, as a result of the interaction between the magnons, there occurs such self-consistent renormalization of the magnon energy and pump-field amplitude as is required to make the instability region disappear.

It turns out that the nature of the steady-state distribution essentially depends on the ratio of the strengths of the interactions conserving and not conserving the magnon number. We proceed from the fact that the

strongest of them is the exchange interaction between the magnons. We also take into consideration the exchange interaction between the magnons and the phonon subsystem, which is regarded as a thermostat, i. e., as being in thermodynamic equilibrium. We shall consider the relativistic interactions to be weak as compared to the exchange interactions, and shall treat their effect on the steady-state distribution as a perturbation. We establish below the conditions under which the corresponding correction to the stationary magnon distribution will be small. As will be shown, it is precisely the relativistic interactions that are responsible for the absorption of energy in the steady-state regime.

The Hamiltonian of the system under consideration by us has the following form:

$$H = H_m + H_p + H_{mm}^{ex} + H_{mp}^{ex} + H_{mm}^r. \quad (1)$$

Here H_m and H_p are the Hamiltonians of the free magnons and phonons, H_m covering the resonance interaction with the pump field:

$$H_m = \sum_k \{ \varepsilon_k a_k^\dagger a_k + \frac{1}{2} (V_k a_k a_{-k} e^{i\omega t} + V_k^* a_k^\dagger a_{-k}^\dagger e^{-i\omega t}) \}, \quad (2)$$

$$H_p = \sum_k E_k b_k^\dagger b_k, \quad (3)$$

where ε_k is the magnon energy, E_k is the phonon ener-